

Fermion Dark Matter Effect on Electroweak Phase Transition

Soudeh Mirzaie¹, Karim Ghorbani¹, Parsa Ghorbani²

¹*Physics Department, Faculty of Science, Arak University, Arak 38156-8-8349, Iran*

²*Physics Department, Faculty of Science, Ferdowsi University of Mashhad, Iran*

Abstract

The addition of extra scalars to the Standard Model (SM) of particle physics enriches the vacuum structure and consequently gives rise to strong first-order phase transitions (EWPT) in the early universe. We raise the question that how the EWPT is affected by the addition of fermions in models beyond the SM, and address this question by studying the EWPT in a dark matter model comprising a singlet scalar and two Dirac fermions. The singlet scalar develops a nonzero vacuum expectation value (VEV), and the lighter fermion plays the role of the dark matter. The model evades the stringent direct detection bounds due to the presence of two fermions. We first show that applying the high-temperature approximation, no first-order phase transition is found. Then we demonstrate that when including the full finite temperature corrections to the effective potential, the first-order phase transition becomes possible, nevertheless, all the phase transitions will be weak. We therefore deduce that the addition of fermions reduces the strength of the EWPT.

1 Introduction

The Standard Model (SM) of particle physics suffers from different theoretical and observational inconsistencies, as such being the problem of dark matter (DM), and the matter-antimatter asymmetry in the universe, as two prominent mysteries of modern physics. To address these problems, it seems inevitable to extend the SM by new degrees of freedom. New fields introduced in the extended models of SM, through different production mechanism (freeze-out, freeze-in, etc) accounts for the observed relic density of DM in the universe, while many direct and indirect constraints must be fulfilled. New fields also reshape the effective potential of the model and may turn the electroweak phase transition (EWPT) from crossover in the SM to a strong first-order EWPT in the extended model, as one of the Sakharov conditions (non-equilibrium) [1] for the baryogenesis. The simplest extension of the SM by a singlet scalar is proved to be an acceptable model of DM. The extra singlet scalar in this model augments the complexity of the vacuum structure of the effective potential which in turn results in the strong first-order EWPT [2–7]. Models beyond the SM (BSM) with more scalar fields possess more complex vacuum structures and will probably always provide strong first-order EWPT. ¹

What happens to the EWPT when the SM is extended with at least one scalar and additional fermions? In this work, we address this question by studying a model of a singlet scalar and two Dirac fermion among which the lighter is the DM candidate. The EWPT and the DM in a model with an extra singlet scalar and a Dirac fermion have already been studied in [12, 13] demonstrating the potential for a strong first-order DM. While the addition of two Dirac fermions [14, 15], helps the model evade the stringent direct detection bounds from LUX and XENONnT, we will assess the impact of these two extra fermions on the EWPT.

In section 2, we introduce the two-fermion scenario and determine the physical masses in the model. In section 3, we analyze the vacuum structure in the high-temperature approximation and study the various phase transition scenarios analytically. In section 4, we present the full finite-temperature effective potential. We then review the theoretical formulation of two-fermion DM model in section 5. In section 6 we present the numerical results. Finally, we conclude in section 7.

2 Model

The Lagrangian of two-fermion model at high temperature where the electroweak (EW) symmetry is unbroken reads,

$$\mathcal{L}_{\text{DM}} = \bar{\chi}_1(i\partial\!\!\!/ - \mu_1)\chi_1 + \bar{\chi}_2(i\partial\!\!\!/ - \mu_2)\chi_2 + g_1 s\bar{\chi}_1\chi_1 + g_2 s\bar{\chi}_2\chi_2 + (g_{12} s\bar{\chi}_1\chi_2 + \text{h.c.}). \quad (1)$$

in which χ_1 and χ_2 are gauge singlet Dirac fermions and s is a real singlet scalar. The potential part of the Lagrangian which incorporates the new singlet scalar and the SM Higgs doublet is given by,

$$V_{\text{tr}}(H, s) = -\frac{1}{2}\mu_s^2 s^2 + \frac{1}{4}\lambda_s s^4 + \lambda_{\text{hs}} s^2 H^\dagger H - \mu_h^2 H^\dagger H + \lambda_h (H^\dagger H)^2. \quad (2)$$

¹This is not generally proved. For two-scalar and 2HDM extension of the SM see e.g. [8–11]

that enjoys the \mathbb{Z}_2 discrete symmetry. The bounded from below condition (BFB), is given by $\lambda_h > 0$, $\lambda_s > 0$, and

$$\lambda_{hs} > 0 \vee (\lambda_{hs} < 0 \wedge \lambda_{hs}^2 \leq \lambda_s \lambda_h). \quad (3)$$

Both scalars take non-zero VEV, ($\langle h \rangle = v$, $\langle s \rangle = w$), so there is a mixing between the Higgs and the singlet scalar

$$\begin{pmatrix} h_1 \\ h_2 \end{pmatrix} = \begin{pmatrix} \cos \theta & \sin \theta \\ -\sin \theta & \cos \theta \end{pmatrix} \begin{pmatrix} h \\ s \end{pmatrix}. \quad (4)$$

The requirement for (v, w) to be the local minimum is given by

$$\mu_h^2 = \lambda_h v^2 + \lambda_{hs} w^2, \quad \mu_s^2 = \lambda_s w^2 + \lambda_{hs} v^2. \quad (5)$$

The scalars' mass matrix,

$$M_S^2 = 2 \begin{pmatrix} \lambda_h v^2 & \lambda_{hs} v w \\ \lambda_{hs} v w & \lambda_s w^2 \end{pmatrix}, \quad (6)$$

should be diagonalized by rotating the field space by the angle θ as in Eq. (4), to get the Higgs mass eigenvalue $m_1 \equiv 125$ GeV, and the singlet scalar physical mass m_2 . The mixing angle in terms of the couplings and the VEVs read,

$$\tan(2\theta) = \frac{2vw\lambda_{hs}}{\lambda_s w^2 - \lambda_h v^2}, \quad (7a)$$

while the parameters λ_h , λ_s and λ_{hs} can be expressed in terms of the physical masses, the VEVs, and the mixing angle as

$$\lambda_{hs} = -\frac{(m_1^2 - m_2^2) \sin(2\theta)}{2vw}, \quad (8a)$$

$$\lambda_h = \frac{(m_1^2 + m_2^2) + (m_1^2 - m_2^2) \cos(2\theta)}{4v^2}, \quad (8b)$$

$$\lambda_s = \frac{(m_1^2 + m_2^2) - (m_1^2 - m_2^2) \cos(2\theta)}{4w^2}. \quad (8c)$$

In addition to scalars, there are mixing among the fermions due to the mixed Yukawa terms $s\bar{\chi}_1\chi_2$ in Eq. (1), after the scalar s undergoes a non-zero VEV. The mass matrix for the fermions becomes,

$$M_F = \begin{pmatrix} -\mu_1 + g_1 w & g_{12} w \\ g_{12} w & -\mu_2 + g_2 w \end{pmatrix}. \quad (9)$$

Again a rotation in the fermions space as

$$\begin{pmatrix} \psi_1 \\ \psi_2 \end{pmatrix} = \begin{pmatrix} \cos \xi & \sin \xi \\ -\sin \xi & \cos \xi \end{pmatrix} \begin{pmatrix} \chi_1 \\ \chi_2 \end{pmatrix}, \quad (10)$$

leads to diagonalization of the mass matrix

$$M_1 = \frac{1}{2}A - \frac{1}{2}\sqrt{A^2 - 4B}, \quad M_2 = \frac{1}{2}A + \frac{1}{2}\sqrt{A^2 - 4B}, \quad (11)$$

with

$$A = (g_1 + g_2)w - (\mu_1 + \mu_2), \quad B = (g_1 w - \mu_1)(g_2 w - \mu_2) - g_{12}^2 w^2. \quad (12)$$

3 Electroweak Phase Transition: High-Temperature

The potential after gauging away three components of the Higgs doublet and at very high temperature reads,

$$V_{\text{tr}}(h, s) = -\frac{1}{2}\mu_s^2 s^2 + \frac{1}{4}\lambda_s s^4 - \frac{1}{2}\mu_h^2 h^2 + \frac{1}{4}\lambda_h h^4 + \frac{1}{2}\lambda_{\text{hs}} h^2 s^2. \quad (13)$$

The dominant one-loop thermal effective potential at high temperature approximation is,

$$V_T^{1\text{-loop}}(h, s; T) \simeq \left(\frac{1}{2}c_h h^2 + \frac{1}{2}c_s s^2 \right) T^2, \quad (14)$$

where the coefficient c_h and c_s are,

$$c_h = \frac{1}{48} (9g^2 + 3g'^2 + 12y_t^2 + 12\lambda_h + 4\lambda_{\text{hs}}), \quad (15a)$$

$$c_s = \frac{1}{12} (\lambda_{\text{hs}} + 3\lambda_s + 2g_1^2 + 2g_2^2 + 4g_{12}^2). \quad (15b)$$

The effective potential can be defined as the sum of the tree-level potential in Eq. (13) and the one-loop thermal contribution in Eq. (14), i.e.,

$$V_{\text{eff}}(h, s) = -\frac{1}{2}\mu_s^2(T) s^2 + \frac{1}{4}\lambda_s s^4 - \frac{1}{2}\mu_h^2(T) h^2 + \frac{1}{4}\lambda_h h^4 + \frac{1}{2}\lambda_{\text{hs}} h^2 s^2, \quad (16)$$

where

$$\mu_h^2(T) = \mu_h^2 - c_h T^2, \quad \mu_s^2(T) = \mu_s^2 - c_s T^2. \quad (17)$$

The first derivatives of the effective potential give the extremum of the field configuration (h, s) . Denoting the extremum point to be (v, w) the conditions are given by,

$$v (-\mu_h^2(T) + \lambda_h v^2 + \lambda_{\text{hs}} w^2) = 0, \quad (18a)$$

$$w (-\mu_s^2(T) + \lambda_s w^2 + \lambda_{\text{hs}} v^2) = 0. \quad (18b)$$

There are four solutions to Eq. (18) being,

$$(v = 0, w = 0), \quad (19a)$$

$$\left(v = 0, w^2 = \frac{\mu_s^2(T)}{\lambda_s} \right), \quad (19b)$$

$$\left(v^2 = \frac{\mu_h^2(T)}{\lambda_h}, w = 0 \right), \quad (19c)$$

$$\left(v^2 = \frac{\lambda_s \mu_h^2(T) - \lambda_{\text{hs}} \mu_s^2(T)}{\lambda_h \lambda_s - \lambda_{\text{hs}}^2}, w^2 = \frac{\lambda_h \mu_s^2(T) - \lambda_{\text{hs}} \mu_h^2(T)}{\lambda_h \lambda_s - \lambda_{\text{hs}}^2} \right). \quad (19d)$$

As the scalar field, s , is a mediator connecting the SM sector to the dark sector comprising two singlet fermions, it can take both zero or non-zero VEV after and before the electroweak phase transition. We therefore consider all four possible one-step phase transition scenarios being as follow,

$$(0, 0) \rightarrow (v, 0), \quad (0, 0) \rightarrow (v, w'), \quad (20a)$$

$$(0, w) \rightarrow (v, 0), \quad (0, w) \rightarrow (v, w'), \quad (20b)$$

where the general solution point (v, w) is given by Eqs. (19) depending on v and w being zero or non-zero. The local minimum conditions for each scenario must be held as part of the necessary criteria for having a first-order phase transition. The second derivatives of the effective potential at the extremum point are given by,

$$V''_{\text{hh}}\Big|_{(v,w)} \equiv \frac{\partial^2 V_{\text{eff}}}{\partial^2 h}\Big|_{(v,w)} = 3\lambda_{\text{h}}v^2 + \lambda_{\text{hs}}w^2 - \mu_{\text{h}}^2(T), \quad (21\text{a})$$

$$V''_{\text{ss}}\Big|_{(v,w)} \equiv \frac{\partial^2 V_{\text{eff}}}{\partial^2 s}\Big|_{(v,w)} = 3\lambda_{\text{s}}w^2 + \lambda_{\text{hs}}v^2 - \mu_{\text{s}}^2(T), \quad (21\text{b})$$

$$V''_{\text{hs}}\Big|_{(v,w)} \equiv \frac{\partial^2 V_{\text{eff}}}{\partial h \partial s}\Big|_{(v,w)} = 2\lambda_{\text{hs}}vw. \quad (21\text{c})$$

Now for the point (v, w) in the field configuration space to be a local minimum we must have,

$$V''_{\text{hh}} > 0, \quad \begin{vmatrix} V''_{\text{hh}} & V''_{\text{hs}} \\ V''_{\text{hs}} & V''_{\text{ss}} \end{vmatrix} > 0. \quad (22)$$

The phase transition triggers below a certain temperature at which the thermal effective potential given in Eq. (16) acquires two degenerate local minima, one of which stays deeper for all temperatures smaller than the critical temperature. The critical temperature then is extracted from,

$$V_{\text{eff}}(v_{\text{sym}} = 0, w_1; T_c) = V_{\text{eff}}(v_{\text{brk}}, w_2; T_c). \quad (23)$$

After the EWPT the VEV of the Higgs particle is non-zero and it goes down to its current value $v_{\text{h}} = 246$ GeV at temperature near $T = 0$. In order for the phase transition to sustain continuously until $T = 0$, the global minimum condition must be imposed on the minimum in the broken phase by,

$$\Delta V_{\text{eff}}(T) \equiv V_{\text{eff}}(0, w_1; T) - V_{\text{eff}}(v_{\text{brk}}, w_2; T) > 0, \quad (24)$$

for $T \leq T_c$. This is equivalent to the condition that T^2 -derivative of $\Delta V_{\text{eff}}(T)$ at T_c be positive. Let us study each scenario in detail.

3.1 Phase Transition $(v = 0, w \neq 0) \rightarrow (v \neq 0, w = 0)$

In this phase transition scenario the singlet scalar develops a non-zero VEV before the EWSB and a zero VEV after the EWSB. The extremum conditions on the thermal effective potential require that $w^2(T) = \mu_{\text{s}}^2(T)/\lambda_{\text{s}}$ and $v^2(T) = \mu_{\text{h}}^2(T)/\lambda_{\text{h}}$. Furthermore the local minimum conditions give

$$\mu_{\text{s}}^2(T) > 0, \quad (25\text{a})$$

$$\frac{\lambda_{\text{hs}}}{\lambda_{\text{s}}}\mu_{\text{s}}^2(T) - \mu_{\text{h}}^2(T) > 0, \quad (25\text{b})$$

and

$$\mu_{\text{h}}^2(T) > 0, \quad (26\text{a})$$

$$\frac{\lambda_{\text{hs}}}{\lambda_{\text{h}}}\mu_{\text{h}}^2(T) - \mu_{\text{s}}^2(T) > 0. \quad (26\text{b})$$

At the critical temperature the thermal effective potential possesses two degenerate minima. Applying the vacua in this scenario into Eq.(23) we have

$$T_c^2 = \frac{\lambda_s \mu_h^2 c_h - \lambda_h \mu_s^2 c_s - \sqrt{\lambda_h \lambda_s} |c_s \mu_h^2 - c_h \mu_s^2|}{\lambda_s \mu_h^2 - \lambda_h \mu_s^2}. \quad (27)$$

This scenario however is not applicable here, because the scalar s must get a non-zero VEV to be a SM-DM mediator.

3.2 Phase Transition $(v = 0, w = 0) \rightarrow (v \neq 0, w = 0)$

This is a phase transition starting from zero VEV for both the Higgs and the scalar at high temperatures and a non-zero VEV for only the Higg field at low temperatures. In high temperature limit we have,

$$\mu_h^2(T) < 0, \quad (28a)$$

$$\mu_s^2(T) < 0, \quad (28b)$$

while at low temperature the local minimum conditions become,

$$\mu_h^2(T) > 0, \quad (29a)$$

$$\frac{\lambda_{hs}}{\lambda_s} \mu_h^2(T) - \mu_s^2(T) > 0. \quad (29b)$$

Eqs. (28) and (26) are manifestly inconsistent, so this type of phase transition for the theory given in (13) does not lead to a first-order phase transition. Moreover from the dark matter point of view this scenario is also not suitable as the scalar field s playing the role of the mediator between DM and SM must have a non-zero VEV after the electroweak phase transition.

3.3 Phase Transition $(v = 0, w = 0) \rightarrow (v \neq 0, w \neq 0)$

In this scenario again field configuration (h, s) undergoes a change in the VEV's from a both zero before the EWPT and both non-zero after the EWPT. The non-zero VEV's after the phase transition must be the solutions given in Eq. (19d). The minimum condition for the point $(0, 0)$ is given by Eq. (28). The conditions for (v, w) reads,

$$3\lambda_h v^2(T) + \lambda_{hs} w^2(T) - \mu_h^2(T) > 0, \quad (30a)$$

$$(3\lambda_h v^2(T) + \lambda_{hs} w^2(T) - \mu_h^2(T)) (3\lambda_s w^2(T) + \lambda_{hs} v^2(T) - \mu_s^2(T)) - 4\lambda_{hs}^2 v^2(T) w^2(T) > 0, \quad (30b)$$

with w and v given by Eq. (19d). The conditions in Eq. (28) and (30), despite similar conditions in subsection 3.2, are not inconsistent. Therefore, we consider more necessary conditions of the first-order phase transition. Rewriting v and w in Eq. (19d) as

$$v^2(T) \equiv \alpha_1 - \beta_1 T^2, \quad w^2(T) \equiv \alpha_2 - \beta_2 T^2, \quad (31)$$

with

$$\alpha_1 = \frac{\lambda_s \mu_h^2 - \lambda_{hs} \mu_s^2}{\lambda_h \lambda_s - \lambda_{hs}^2}, \quad \beta_1 = \frac{\lambda_s c_h - \lambda_{hs} c_s}{\lambda_h \lambda_s - \lambda_{hs}^2}, \quad (32a)$$

$$\alpha_2 = \frac{\lambda_h \mu_s^2 - \lambda_{hs} \mu_h^2}{\lambda_h \lambda_s - \lambda_{hs}^2}, \quad \beta_2 = \frac{\lambda_h c_s - \lambda_{hs} c_h}{\lambda_h \lambda_s - \lambda_{hs}^2}, \quad (32b)$$

the critical temperature is as follows

$$T_c^2 = \frac{c_h \lambda_s \mu_h^2 + c_s \lambda_h \mu_s^2 - c_s \lambda_{hs} \mu_h^2 - c_h \lambda_{hs} \mu_s^2 \pm |c_s \mu_h^2 - c_h \mu_s^2| \sqrt{\lambda_{hs}^2 - \lambda_h \lambda_s}}{c_s^2 \lambda_h - 2c_h c_s \lambda_{hs} + c_h^2 \lambda_s}, \quad (33)$$

which requires $\lambda_h \lambda_s < \lambda_{hs}^2$. By looking at the BFB condition in Eq. (3), this means that λ_{hs} can only be positive.

The local minimum conditions in Eqs. (28) and (30) are held for all $T \leq T_c$ if they are satisfied at $T = 0$ and $T = T_c$,

$$\mu_h^2 < 0, \quad \mu_h^2 - c_h T_c^2 < 0, \quad (34a)$$

$$\mu_s^2 < 0, \quad \mu_s^2 - c_s T_c^2 < 0, \quad (34b)$$

and

$$3\lambda_h \alpha_1 + \lambda_{hs} \alpha_2 - \mu_h^2 > 0, \quad (35a)$$

$$(3\lambda_h \alpha_1 + \lambda_{hs} \alpha_2 - \mu_h^2) (3\lambda_s \alpha_2 + \lambda_{hs} \alpha_1 - \mu_s^2) - 4\lambda_{hs}^2 \alpha_1 \alpha_2 > 0, \quad (35b)$$

$$3\lambda_h \alpha_1 + \lambda_{hs} \alpha_2 - \mu_h^2 + (c_h - 3\lambda_h \beta_1 - \lambda_{hs} \beta_2) T_c^2 > 0, \quad (35c)$$

$$\begin{aligned} & (3\lambda_h \alpha_1 + \lambda_{hs} \alpha_2 - \mu_h^2 + (c_h - 3\lambda_h \beta_1 - \lambda_{hs} \beta_2) T_c^2) \\ & \times (3\lambda_s \alpha_2 + \lambda_{hs} \alpha_1 - \mu_s^2 + (c_s - 3\lambda_s \beta_2 - \lambda_{hs} \beta_1) T_c^2) - 4\lambda_{hs}^2 (\alpha_1 - \beta_1 T_c^2) (\alpha_2 - \beta_2 T_c^2) > 0. \end{aligned} \quad (35d)$$

The global minimum condition for the point (v, w) reads

$$c_h \lambda_s \mu_h^2 + c_s \lambda_h \mu_s^2 - c_s \lambda_{hs} \mu_h^2 - c_h \lambda_{hs} \mu_s^2 + (2c_h c_s \lambda_{hs} - c_s^2 \lambda_h - c_h^2 \lambda_s) T_c^2 > 0. \quad (36)$$

3.4 Phase Transition $(v = 0, w \neq 0) \rightarrow (v \neq 0, w' \neq 0)$

The phase transition in this scenario is from the minimum $(0, w)$ with $w^2 = \mu_s^2(T)/\lambda_s$ at high temperature into the minimum (v, w') with

$$v^2 = \frac{\lambda_s \mu_h^2(T) - \lambda_{hs} \mu_s^2(T)}{\lambda_h \lambda_s - \lambda_{hs}^2}, \quad w'^2 = \frac{\lambda_h \mu_s^2(T) - \lambda_{hs} \mu_h^2(T)}{\lambda_h \lambda_s - \lambda_{hs}^2} \quad (37)$$

at low temperature. The first-order conditions for the point $(0, w)$ reads,

$$\frac{\lambda_{hs}}{\lambda_s} \mu_s^2(T) - \mu_h^2(T) > 0, \quad (38a)$$

$$\mu_s^2(T) > 0. \quad (38b)$$

The same conditions for the minimum (v, w') becomes,

$$\frac{\lambda_h (\lambda_s \mu_h^2(T) - \lambda_{hs} \mu_s^2(T))}{\lambda_h \lambda_s - \lambda_{hs}^2} > 0, \quad (39a)$$

$$\frac{(\lambda_h \mu_s^2(T) - \lambda_{hs} \mu_h^2(T)) (\lambda_s \mu_h^2(T) - \lambda_{hs} \mu_s^2(T))}{\lambda_h \lambda_s - \lambda_{hs}^2} > 0. \quad (39b)$$

The critical temperature for this scenarios is given by

$$T_c^2 = \frac{a \pm \sqrt{a^2 + bc}}{b} \quad (40)$$

where

$$a = c_h \alpha_1 \lambda_s + c_s (\alpha_2 \lambda_s - \mu_s^2) - \lambda_s (\alpha_1 \beta_1 \lambda_h + \alpha_2 \beta_1 \lambda_{hs} + \alpha_1 \beta_2 \lambda_{hs} + \alpha_2 \beta_2 \lambda_s - \beta_1 \mu_h^2 - \beta_2 \mu_s^2), \quad (41a)$$

$$b = -c_s^2 + \lambda_s (2c_h \beta_1 + 2c_s \beta_2 - \lambda_h \beta_1^2 - 2\lambda_{hs} \beta_1 \beta_2 - \beta_2^2), \quad (41b)$$

$$c = \lambda_s \alpha_1 (\lambda_h \alpha_1 + 2\lambda_{hs} \alpha_2 - 2\mu_h^2) + (\mu_s^2 - \lambda_s \alpha_2)^2. \quad (41c)$$

Both Eqs. (38) and (39) must be satisfied for all $T \leq T_c$, which means they must be satisfied for $T = 0$ and $T = T_c$, i.e.

$$\frac{\lambda_{hs}}{\lambda_s} \mu_s^2 - \mu_h^2 > 0, \quad (42a)$$

$$\mu_s^2 > 0, \quad (42b)$$

$$\frac{\lambda_{hs}}{\lambda_s} (\mu_s^2 - c_s T_c^2) - (\mu_h^2 - c_h T_c^2) > 0, \quad (42c)$$

$$\mu_s^2 - c_s T_c^2 > 0, \quad (42d)$$

and

$$\frac{\lambda_h (\lambda_s \mu_h^2 - \lambda_{hs} \mu_s^2)}{\lambda_h \lambda_s - \lambda_{hs}^2} > 0, \quad (43a)$$

$$\frac{(\lambda_h \mu_s^2 - \lambda_{hs} \mu_h^2) (\lambda_s \mu_h^2 - \lambda_{hs} \mu_s^2)}{\lambda_h \lambda_s - \lambda_{hs}^2} > 0. \quad (43b)$$

Now, the global minimum condition takes the following form,

$$c_s \alpha_2 \lambda_s - c_s \mu_s^2 + c_h \alpha_1 \lambda_s - \alpha_2 \beta_1 \lambda_{hs} - \alpha_1 \beta_1 \lambda_h - \alpha_1 \beta_2 \lambda_{hs} - \alpha_2 \beta_2 \lambda_s + \beta_1 \mu_h^2 + \beta_2 \mu_s^2 + (c_s^2 - 2c_s \beta_2 \lambda_s - 2\beta_1 \lambda_s + \beta_1^2 \lambda_h + 2\beta_1 \beta_2 \lambda_{hs} + \beta_2^2 \lambda_s) T_c^2 > 0. \quad (44)$$

4 Electroweak Phase Transition: Finite-Temperature

The finite temperature effective potential beside the tree-level potential consists of thermal contributions and zero-temperature Coleman-Weinberg one-loop correction,

$$V_{\text{eff}}(h, s; T) = V_{\text{tr}}(h, s) + V_{\text{CW}}(h, s) + V_T(h, s; T). \quad (45)$$

For the two-fermion DM model with an extra singlet scalar and two singlet Dirac fermions, the one-loop Coleman-Weinberg contribution $V_{\text{CW}}(h, s)$ using the on-shell renormalization scheme and cut-off regularization reads,

$$V_{\text{CW}} = \frac{1}{64\pi^2} \sum_i (-1)^{f_i} g_i \left[M_i^4(h, s) \left(\log \frac{M_i^2(h, s)}{M_{i_{\text{EW}}}^2} - \frac{3}{2} \right) - 2M_i^2(h, s)M_{i_{\text{EW}}}^2 \right], \quad (46)$$

where $M_i(h, s)$ are scalar-field-dependent masses of all particles in the model

$$M_{h,s}^2 = \begin{pmatrix} 3\lambda_h h^2 + \lambda_{hs} s^2 - \mu_h^2 & 2\lambda_{hs} h s, \\ 2\lambda_{hs} h s & 3\lambda_s s^2 + \lambda_{hs} h^2 - \mu_s^2 \end{pmatrix}, \quad (47a)$$

$$M_{\psi_1, \psi_2}^2 = \begin{pmatrix} -\mu_1 + g_1 s & g_{12} s \\ g_{12} s & -\mu_2 + g_2 s \end{pmatrix}, \quad (47b)$$

$$M_W^2 = \frac{1}{4} g^2 h^2, \quad (47c)$$

$$M_Z^2 = \frac{1}{4} (g^2 + g'^2) h^2, \quad (47d)$$

$$M_t^2 = \frac{1}{2} y_t^2 h^2. \quad (47e)$$

For bosons $f_i = 0$ and for fermions $f_i = 1$. Also $M_{i_{\text{EW}}}$ stands for the masses in the electroweak vacuum. The thermal one-loop potential V_T is given by

$$V_T = \frac{T^4}{2\pi^2} \sum_i (-1)^{f_i} g_i J_{F,B} \left(\frac{M_i}{T} \right), \quad (48)$$

where

$$J_{F,B}(x) = \int_0^\infty y^2 \log \left(1 \pm e^{-\sqrt{x^2 + y^2}} \right) dy, \quad (49)$$

where M_i is the field dependent mass, and B (F) stands for boson (fermion) and corresponds to the minus (plus) sign. In order to include the contributions of daisy diagrams to prevent the IR divergence at high temperature we need to modify the total effective potential by replacing the masses in V_{CW} and V_T by thermally-corrected masses as

$$M_{h,s}^2 \rightarrow M_{h,s}^2 + \begin{pmatrix} \Pi_h(T) & 0 \\ 0 & \Pi_s(T) \end{pmatrix}, \quad (50a)$$

$$M_W^2(h) \rightarrow M_W^2(h) + \Pi_W(T), \quad (50b)$$

$$M_{Z,\gamma}^2(h) = \begin{pmatrix} \frac{1}{4} g^2 h^2 + \frac{11}{6} g^2 T^2 & -\frac{1}{4} g g' h^2 \\ -\frac{1}{4} g g' h^2 & \frac{1}{4} g'^2 h^2 + \frac{11}{6} g'^2 T^2 \end{pmatrix}, \quad (50c)$$

with the thermal mass contributions $\Pi_i(T)$

$$\Pi_h(T) = \frac{1}{48} (9g^2 + 3g'^2 + 12y_t^2 + 24\lambda_h + 2\lambda_{hs}) T^2, \quad (51a)$$

$$\Pi_s(T) = \frac{1}{12} (3\lambda_s + 2\lambda_{hs}) T^2, \quad (51b)$$

$$\Pi_W(T) = \frac{11}{6} g^2 T^2. \quad (51c)$$

5 Two-Fermion Dark Matter

In the two-fermion model after diagonalization of the fermion mass matrix by rotating the fermions space from (χ_1, χ_2) to (ψ_1, ψ_2) with physical mass splitting $\delta = M_2 - M_1$ the lighter fermion, ψ_1 , is taken as the DM candidate. The singlet scalar h_2 , plays the role of the mediator between the dark and visible sectors. This model is interestingly able to evade the direct detection strong bounds [14].

5.1 Dark Matter Abundance

The DM fermion annihilation into SM fermions occurs via s -channel and into the Higgs and the singlet scalar goes through the t - and u -channels. Moreover, due to the fermion mixing term in the model, there is also coannihilation into the SM fermions and the scalars. To take into account the effect of the coannihilation in the DM number density the Boltzmann equation can be solved with an effective coannihilation cross section [16, 17]

$$\frac{dn}{dt} + 3nH = -\langle\sigma_{\text{eff}}v\rangle(n^2 - n_{\text{eq}}^2), \quad (52)$$

where $n = n_1 + n_2$ is total number density incorporating the DM particle ψ_1 and the heavier fermion ψ_2 . Also H stands for the Hubble parameter and σ_{eff} is the effective DM annihilation cross section given by

$$\sigma_{\text{eff}} = \frac{4}{g_{\text{eff}}^2} \left(\sigma_{11} + \sigma_{22} \left(1 + \frac{\delta}{M_1}\right)^3 e^{-2\delta/T} + 2\sigma_{12} \left(1 + \frac{\delta}{M_1}\right)^{3/2} e^{-\delta/T} \right), \quad (53)$$

with σ_{ij} being the (co)annihilation cross section for $\psi_i\psi_j \rightarrow SM$, and g_{eff} being the effective internal degrees of freedom given by

$$g_{\text{eff}} = 2 + 2 \left(1 + \frac{\delta}{M_1}\right)^{3/2} e^{-\delta/T}. \quad (54)$$

The bracket $\langle \rangle$ means the thermal average. To solve the above Boltzmann equation we use the `MicrOMEGAs` package. The free parameters in the model are the masses m_2, M_1, M_2 , the couplings g_1, g_2, g_{12} , and the mixing angle θ and the scalar VEV, w . The Higgs mass and the Higgs VEV take their experimental values $m_1 = 125$ GeV and $v_0 = 246$ GeV.

5.2 Direct Detection

The direct detection (DD) of the DM through DM scattering off the nucleus has become more stringent than ever in the recent DD experiments [18–21], which brings the lower limits of the DM-nucleon cross section almost down to the neutrino floor [22]. Therefore many DM models including the singlet fermion DM are already ruled out. However, similar to the case of two-scalar scenario, the two-fermion model evades the strong DD limits as explained in [14]. The DM-nucleon cross section is deduced from a t -channel interaction among the DM fermion and quarks inside the nucleon $\psi_1 q \rightarrow \psi_1 q$, mediated by the Higgs and the singlet scalar

$$\mathcal{L} = c_q \bar{\psi}_1 \psi_1 \bar{q} q, \quad (55)$$

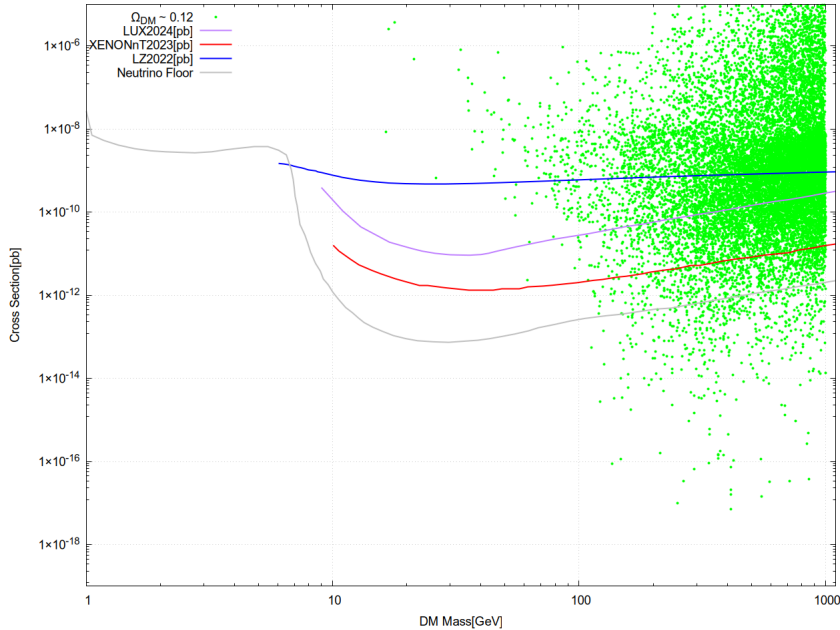


Figure 1: Shown is the DM mass vs. DM-nucleon cross section when the DM relic density is constrained to $\Omega_{\text{DM}}h^2 \sim 0.12$. The DM-nucleon direct detection bounds XENONnT, LZ and LUX, exclude part of the parameter space.

where the coupling is given by

$$c_q = g_1 \sin(2\theta) \frac{m_q}{2v_0} \left(\frac{1}{m_h^2} - \frac{1}{m_s^2} \right). \quad (56)$$

The spin-independent (SI) DM-nucleon scattering cross section at zero momentum transfer is given

$$\sigma_{\text{SI}}^N = \frac{4\mu_N^2 c_N^2}{\pi}, \quad (57)$$

where μ_N is the reduced mass of the DM the nucleon and the nucleon effective coupling c_N , is expressed in terms of the quark coupling c_q and scalar form factors [23, 24],

$$c_N = m_N \left(\sum_{q=u,d,s} f_{Tq}^N \frac{c_q}{m_q} + \frac{2}{27} f_{Tg}^N \sum_{q=c,b,t} \frac{c_q}{m_q} \right), \quad (58)$$

with scalar form factors being

$$f_u^p = 0.0153, \quad f_d^p = 0.0191, \quad f_s^p = 0.0447. \quad (59)$$

The numerical calculations again is done using the package `MicrOMEGAs`. We confront the model against a combination of the constraints of the DD bounds, DM relic abundance, and the conditions for a strongly first-order phase transition.

6 Numerical Results

The independent free parameters in the model are the scalar VEV, w , the scalar mass m_s , the mixing angle θ , the DM fermions' masses M_1, M_2 , and the Yukawa couplings g_1 ,

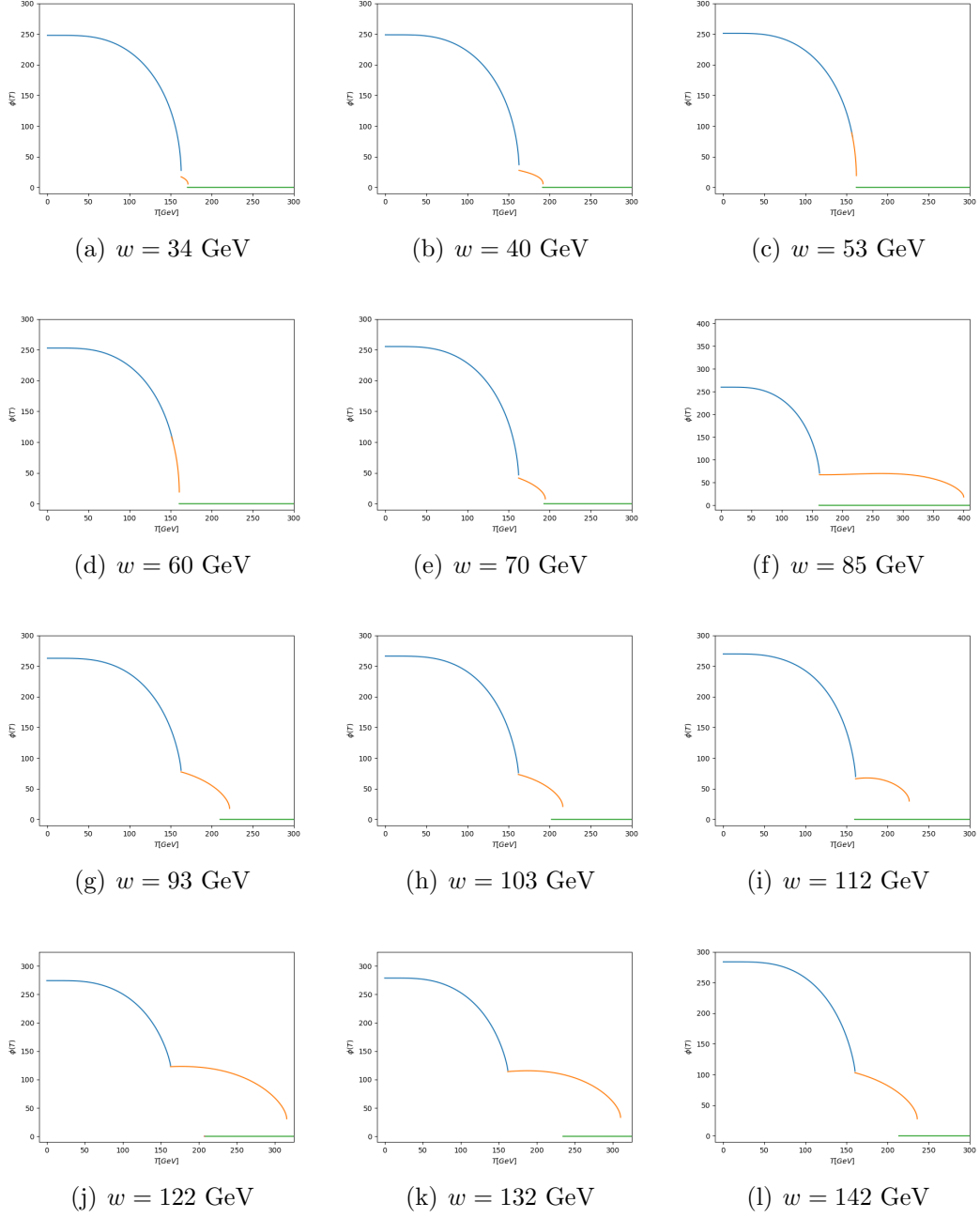


Figure 2: Show are two-step first-order electroweak phase transitions for different scalar VEVs. All the phase transitions are weak.

$w(\text{GeV})$	Phase Transition – Step 1				Phase Transition – Step 2				
	$T_n(\text{GeV})$	$T_c(\text{GeV})$	From: (v, w)	To: (v, w)	$T_n(\text{GeV})$	$T_c(\text{GeV})$	From: (v, v)	To: (v, w)	$v(T_n)/T_n$
33.87	170.98	170.99	(0, 0)	(0, 7.05)	162.83	162.84	(0, 17.10)	(23.79, 17.11)	0.146
40.00	191.86	191.87	(0, 0)	(0, 7.51)	162.76	162.77	(0, 27.70)	(24.44, 27.7)	0.150
53.09	162.04	162.05	(0, 0)	(23, 0)	157.36	157.38	(82, 0)	(82.58, 8.52)	0.145
60.57	160.56	160.57	(0, 0)	(23, 0)	152.3	152.4	(100, 0)	(102.8, 12.3)	0.146
70.07	194.47	194.5	(0, 0)	(0, 10)	162.24	162.25	(0, 41)	(23.71, 41.81)	0.146
85.90	396.3	396.7	(0, 0)	(0, 28)	162.29	162.3	(0, 67)	(23.71, 67.40)	0.146
93.34	220.4	220.6	(0, 0)	(0, 25)	162.71	162.72	(0, 77)	(23.6, 77.5)	0.146
103.0	214.1	214.4	(0, 0)	(0, 29)	161.98	161.99	(0, 73)	(23.7, 73.5)	0.146
112.1	222.0	222.9	(0, 0)	(0, 42)	161.07	161.08	(0, 66)	(24, 66.9)	0.149
122.40	311.4	312.1	(0, 0)	(0, 48)	162.77	162.78	(0, 120)	(23.7, 122.7)	0.149
132.30	305.6	306.4	(0, 0)	(0, 50)	161.89	161.90	(0, 110)	(23.9, 114.2)	0.145
142.40	233.5	233.9	(0, 0)	(0, 40)	160.411	160.419	(0, 100)	(23.8, 103.2)	0.147

Table 1: The vacuum structure, the critical and nucleation temperature of two-step electroweak phase transitions for different values of the scalar VEV corresponding to phase transition diagrams in Figure 2 are shown.

g_2, g_{12} . In our scan, we restricted the scalar-Higgs mixing angle to comply the LHC14 constraint $\sin^2 \theta \lesssim 0.02$ [25]. We utilized the `MicrOMEGAs` package [26], to find the viable parameter space satisfying the observed dark matter relic density $\Omega_{\text{DM}} h^2 \sim 0.12$ [27, 28], and to calculate the DM-nucleon scattering cross section. Figure 1 shows the viable parameter space for DM when the observed relic density constraint is satisfied. After applying the direct detection bounds from XENONnT [21], LZ [20] and LUX [18] experiments, it is evident from this figure that DM mass heavier than around 40 GeV evades these constraints. We take only the viable parameter space below the LZ bound and above the neutrino floor to examine the electroweak phase transition. The numerical calculations confirms the analytic results in section 3; no first-order phase transition takes place using the high-temperature approximation. To evaluate numerically the phase transition at finite-temperature described in section 4, we used the package `CosmoTransitions`[29]. We examined the electroweak phase transition for all the points within the viable parameter space evading the direct detection and the DM relic density constraints depicted in Figure 1.

A selected number of benchmarks with different values of the scalar VEV, from $w = 33$ GeV to $w = 142$ GeV, are shown in Figure 2. First, as seen in this figure, for all the benchmarks (and for the whole viable parameter space), the phase transition occurs through two steps. For all benchmarks, the phase transition starts from the symmetric phase $(0, 0)$ at higher temperatures and ends to either $(v, 0)$ or $(0, w)$ vacuum structure

$w(\text{GeV})$	$M_1(\text{GeV})$	$M_2(\text{GeV})$	$m_s(\text{GeV})$	λ_h	λ_{hs}	λ_s	g_1	g_2	g_{12}	$\sin \theta$
33.87	409.10	561.40	144.9	0.1291	0.0214	9.152	1.244	1.994	-0.208	0.03
40.00	596.7	871.6	164.2	0.1291	0.0172	8.42	1.072	0.9554	-0.873	0.01
53.09	836.20	943.50	86.59	0.1290	-0.0212	1.332	1.154	0.348	0.799	0.03
60.57	349.80	558.30	85.22	0.1295	-0.0516	0.993	0.130	1.487	0.971	0.09
70.07	167.30	287.80	95.62	0.1290	-0.0153	0.932	0.254	1.191	0.690	0.05
85.90	685.00	838.20	85.90	0.1290	-0.0153	0.532	0.856	1.180	0.953	0.04
93.34	175.00	358.90	67.55	0.1291	-0.0034	0.262	0.100	0.243	0.749	0.006
103.00	142.80	400.20	67.50	0.1290	-0.0156	0.215	0.147	1.877	0.781	0.03
112.10	320.70	435.20	48.19	0.1289	-0.0218	0.093	0.039	1.325	-0.883	0.04
122.40	337.90	508.60	75.37	0.1291	-0.0053	0.189	0.299	0.904	0.886	0.01
132.30	369.90	502.40	74.76	0.1288	-0.0181	0.160	0.414	1.122	0.864	0.06
142.40	91.02	373.40	86.40	0.1285	-0.2257	0.1859	0.3588	1.052	0.689	0.09

Table 2: The values of the free parameters in the model corresponding to the two-step phase transitions shown in Figure 2.

at lower temperature in the first step. In the second step, this vacuum structure changes ultimately to the vacuum structure (v, w) , which is required by our original assumption that both the Higgs and singlet scalar develop non-zero VEVs at zero temperature. Secondly, none of the phase transitions are strong in either steps. The corresponding critical and nucleation temperatures, and the phase transition strength are given for each step in Table 1. In Table 2, the parameters and couplings used in the model corresponding to each phase transition diagram in Figure 2 is shown. The DM mass (singlet scalar mass) ranges from $M_1 = 91$ GeV ($m_s = 48$ GeV) to $M_1 = 836$ GeV ($m_s = 164$ GeV). The Higgs-scalar coupling λ_{hs} , as well as the mixing angle $\sin \theta$, take always very small values. Comparing the current DM fermion model with the DM scalar model, the remarkable result is that the effect of including fermions as DM candidate weakens the electroweak phase transition considerably.

7 Conclusion

It is known that extending the Standard Model of particle physics even by a single scalar changes the type of the electroweak phase transition (EWPT) from crossover to strongly first-order phase transition[4]. Consequently, adding more scalars could maintain or increase the strength of the first-order phase transition [8]. In this work, we investigated the effect of fermion dark matter in the EWPT. To this end, we extended the singlet scalar model by two Dirac fermions, one of them being the DM candidate, to compare the phase transition behavior of this model with that of the singlet scalar model. It is argued already that the addition of a single Dirac fermion is not enough to evade the thermal dark matter (DM) constraints [14]. To begin, we have presented an analytic calculation of the phase transition within the high-temperature approximation formulation. Two phase transitions $(0, 0) \rightarrow (v, 0)$ and $(0, w) \rightarrow (v, 0)$ are not of our interest because the singlet scalar is required to

gain a non-zero VEV to obtain the correct relic density for the DM fermion in the freeze-out mechanism. We have shown that no phase transition with the structures $(0, 0) \rightarrow (v, w)$ or $(0, w) \rightarrow (v, w)$ occurs at high temperature. Using the full thermal corrections of the effective potential at finite temperature, and taking into account the observed DM relic density, and DM direct detection constraints, we have demonstrated that although two-step first-order phase transition is possible in the presence of DM fermion, but these phase transitions can never be strong. Therefore, we concluded that the addition of fermions in the extended theories of the SM, if not changing the type, at least weaken the strength of the EWPT.

References

- [1] A. D. Sakharov. Violation of CP Invariance, C asymmetry, and baryon asymmetry of the universe. *Pisma Zh. Eksp. Teor. Fiz.*, 5:32–35, 1967.
- [2] Wei Chao, Xiu-Fei Li, and Lei Wang. Filtered pseudo-scalar dark matter and gravitational waves from first order phase transition. *JCAP*, 06:038, 2021.
- [3] Cheng-Wei Chiang, Da Huang, and Bo-Qiang Lu. Electroweak phase transition confronted with dark matter detection constraints. *JCAP*, 01:035, 2021.
- [4] Karim Ghorbani and Parsa Hossein Ghorbani. Strongly First-Order Phase Transition in Real Singlet Scalar Dark Matter Model. *J. Phys. G*, 47(1):015201, 2020.
- [5] Parsa Ghorbani. Vacuum structure and electroweak phase transition in singlet scalar dark matter. *Phys. Dark Univ.*, 33:100861, 2021.
- [6] Ankit Beniwal, Marek Lewicki, Martin White, and Anthony G. Williams. Gravitational waves and electroweak baryogenesis in a global study of the extended scalar singlet model. *JHEP*, 02:183, 2019.
- [7] Simone Biondini, Philipp Schicho, and Tuomas V. I. Tenkanen. Strong electroweak phase transition in t-channel simplified dark matter models. *JCAP*, 10:044, 2022.
- [8] Karim Ghorbani and Parsa Hossein Ghorbani. A Simultaneous Study of Dark Matter and Phase Transition: Two-Scalar Scenario. *JHEP*, 12:077, 2019.
- [9] Shinya Kanemura and Masanori Tanaka. Strongly first-order electroweak phase transition by relatively heavy additional Higgs bosons. *Phys. Rev. D*, 106(3):035012, 2022.
- [10] Songtao Liu and Lei Wang. Spontaneous CP violation electroweak baryogenesis and gravitational wave through multistep phase transitions. *Phys. Rev. D*, 107(11):115008, 2023.
- [11] Dilip Kumar Ghosh, Koustav Mukherjee, and Shourya Mukherjee. Electroweak phase transition in two scalar singlet model with pNGB dark matter. *JHEP*, 01:078, 2025.
- [12] Malcolm Fairbairn and Robert Hogan. Singlet Fermionic Dark Matter and the Electroweak Phase Transition. *JHEP*, 09:022, 2013.

- [13] Parsa Hossein Ghorbani. Electroweak Baryogenesis and Dark Matter via a Pseudoscalar vs. Scalar. *JHEP*, 08:058, 2017.
- [14] Karim Ghorbani. Split fermionic WIMPs evade direct detection. *JHEP*, 11:086, 2018.
- [15] Khadije Rahi Maleki and Karim Ghorbani. Loop enhancement of direct detection cross section in a fermionic dark matter model. *Eur. Phys. J. C*, 83(6):473, 2023.
- [16] Kim Griest and David Seckel. Three exceptions in the calculation of relic abundances. *Phys. Rev. D*, 43:3191–3203, May 1991.
- [17] Joakim Edsjo and Paolo Gondolo. Neutralino relic density including coannihilations. *Phys. Rev. D*, 56:1879–1894, 1997.
- [18] D. S. Akerib et al. Results from a search for dark matter in the complete LUX exposure. *Phys. Rev. Lett.*, 118(2):021303, 2017.
- [19] Yue Meng et al. Dark Matter Search Results from the PandaX-4T Commissioning Run. *Phys. Rev. Lett.*, 127(26):261802, 2021.
- [20] J. Aalbers et al. First Dark Matter Search Results from the LUX-ZEPLIN (LZ) Experiment. *Phys. Rev. Lett.*, 131(4):041002, 2023.
- [21] E. Aprile et al. First Dark Matter Search with Nuclear Recoils from the XENONnT Experiment. *Phys. Rev. Lett.*, 131(4):041003, 2023.
- [22] Julien Billard et al. Direct detection of dark matter—APPEC committee report*. *Rept. Prog. Phys.*, 85(5):056201, 2022.
- [23] John R. Ellis, Keith A. Olive, and Christopher Savage. Hadronic Uncertainties in the Elastic Scattering of Supersymmetric Dark Matter. *Phys. Rev. D*, 77:065026, 2008.
- [24] Andreas Crivellin, Martin Hoferichter, and Massimiliano Procura. Accurate evaluation of hadronic uncertainties in spin-independent WIMP-nucleon scattering: Disentangling two- and three-flavor effects. *Phys. Rev. D*, 89:054021, 2014.
- [25] Sally Dawson et al. Working Group Report: Higgs Boson. In *Snowmass 2013: Snowmass on the Mississippi*, 10 2013.
- [26] G. Alguero, G. Belanger, F. Boudjema, S. Chakraborti, A. Goudelis, S. Kraml, A. Mjallal, and A. Pukhov. micrOMEGAs 6.0: N-component dark matter. *Comput. Phys. Commun.*, 299:109133, 2024.
- [27] G. Hinshaw et al. Nine-year wilkinson microwave anisotropy probe (wmap) observations: Cosmological parameter results. *Astrophys.J.Suppl.*, 208:19, 2013.
- [28] N. Aghanim et al. Planck 2018 results. VI. Cosmological parameters. *Astron. Astrophys.*, 641:A6, 2020. [Erratum: *Astron.Astrophys.* 652, C4 (2021)].
- [29] Carroll L. Wainwright. CosmoTransitions: Computing Cosmological Phase Transition Temperatures and Bubble Profiles with Multiple Fields. *Comput. Phys. Commun.*, 183:2006–2013, 2012.